*Sensors & Transducers, Vol. 25, Special Issue, December 2013, pp. 9-16*

www.sensorsportal.com

**Sensors & Transducers**



*http://www.sensorsportal.com*

# Frequency Characteristics Analysis of Vibration System for Planetary Wheeled Vehicle

**Yuchuan Lu, Zhiqi Du, Bo Su, Lei Jiang, Guoxuan Lu, Zhijie Zhang**
China North Vehicle Research Institute
Tel.: +86-13511076894
E-mail: luych702502@126.com

*Received: 16 September 2013 /Accepted: 15 October 2013 /Published: 23 December 2013*

**Abstract**: In order to consider the sink effect that caused by the mental wheels when the planetary wheeled vehicle is driving on the soft soil, 7-DOF spatial vibration model of the whole vehicle is rebuilt. Differential equations of this system are obtained by Lagrangian equations. Then the mathematical expressions of the frequency characteristics are derived, which respectively belong to the motion of the body center-of-mass, the dynamic deflections of the four suspensions and the relative dynamic loadings of the four equivalent wheels. Finally, the corresponding amplitude-frequency characteristic curves and phase-frequency characteristic ones are presented by MATLAB, and the frequency characteristics of the whole vehicle vibration system are also analyzed. Simulation results show that the designed parameters of the vehicle are reasonable. The analytic expressions solved above have a certain guiding significance in theory for vehicle vibration study, vibration control and vehicle-related parameters optimization. *Copyright © 2013 IFSA.*

**Keywords:** Planetary, Spatial vibration, Dynamic deflection, Relative dynamic loadings, Amplitude frequency characteristic, Phase frequency characteristic.

## 1. Introduction

Planetary wheeled vehicle has certain advantages while operating in the off-road environment [1]. In this paper, in order to solve the sink effect of the mental wheels while the planetary wheeled vehicles are operating on the soft soil, the vibration model in the literature [2] is improved. In this model, the soil soft characteristics and the wheels sinking are transfer to damping and each planetary gear train wheels is equivalent to a single wheel with damping. Because of the soft soil and the rigid metal wheels, the road can be regarded as hard-surface without any total effect changed. With the advantages of the equivalent and conversion, the road roughness incentive is regarded as point incentive for each wheel which facilitates the analysis of the problem, but also simplifies the mathematical processing.

## 2. Differential Equations for Vibration System

A new 7-DOF spatial vibration model for the planetary wheeled vehicle is shown in Fig. 1. The generalized coordinates of this vibration system is defined as $\{Z\}=\{z_M \quad \theta \quad \varphi \quad z_{wfl} \quad z_{wfr} \quad z_{wrl} \quad z_{wrr}\}^T$. The physical meaning of each coordinate is stated as follows: vertical displacement of the body center-of-mass, the angular displacement according to positive x-axis rotation of the body, the angular displacement according to positive y-axis rotation of the body, the vertical displacements of the left front equivalent wheel, right front equivalent wheel, left rear equivalent wheel, right rear equivalent wheel. The generalized coordinate origin is the static equilibrium position of each DOF while the vehicle is on a

horizontal static plane. According to Lagrange equations of the vibration system,

$$\frac{d}{dt}\left(\frac{\partial L}{\partial \dot{q}_i}\right)-\frac{\partial L}{\partial q_i}+\frac{\partial \psi}{\partial \dot{q}_i}=0,\quad i=1,2,..,7$$

differential equations in matrix form for the vibration system is obtained:

$$[M]\{\ddot{Z}\}+[C]\{\dot{Z}\}+[K]\{Z\}=\{F\}, \qquad (1)$$

where the mass matrix is:

$$[M]=\begin{pmatrix} M & 0 & 0 & 0 & 0 & 0 & 0 \\ 0 & I_\theta & 0 & 0 & 0 & 0 & 0 \\ 0 & 0 & I_\varphi & 0 & 0 & 0 & 0 \\ 0 & 0 & 0 & m_{wf} & 0 & 0 & 0 \\ 0 & 0 & 0 & 0 & m_{wf} & 0 & 0 \\ 0 & 0 & 0 & 0 & 0 & m_{wr} & 0 \\ 0 & 0 & 0 & 0 & 0 & 0 & m_{wr} \end{pmatrix}$$

the damping matrix is:

$$[C]=\begin{pmatrix} 2(c_f+c_r) & (n-m)(c_f+c_r) & 2(-ac_f+bc_r) & -c_f\frac{r_{f2}}{r_{f1}} & -c_f\frac{r_{f2}}{r_{f1}} & -c_r\frac{r_{r2}}{r_{r1}} & -c_r\frac{r_{r2}}{r_{r1}} \\ & (n^2+m^2)(c_f+c_r) & (n-m)(-ac_f+bc_r) & -nc_f\frac{r_{f2}}{r_{f1}} & mc_f\frac{r_{f2}}{r_{f1}} & -nc_r\frac{r_{r2}}{r_{r1}} & mc_r\frac{r_{r2}}{r_{r1}} \\ & & 2(a^2c_f+b^2c_r) & ac_f\frac{r_{f2}}{r_{f1}} & ac_f\frac{r_{f2}}{r_{f1}} & -bc_r\frac{r_{r2}}{r_{r1}} & -bc_r\frac{r_{r2}}{r_{r1}} \\ & & & c_f\frac{r_{f2}^2}{r_{f1}^2}+c_{fw} & 0 & 0 & 0 \\ & & sym & & c_f\frac{r_{f2}^2}{r_{f1}^2}+c_{fw} & 0 & 0 \\ & & & & & c_r\frac{r_{r2}^2}{r_{r1}^2}+c_{rw} & 0 \\ & & & & & & c_r\frac{r_{r2}^2}{r_{r1}^2}+c_{rw} \end{pmatrix}$$

the stiffness matrix is:

$$[K]=\begin{pmatrix} \left\langle 2(k_f\frac{\sin^2\alpha}{r_{f2}^2}+k_r\frac{\sin^2\beta}{r_{r2}^2})\right\rangle & \left\langle (n-m)(k_f\frac{\sin^2\alpha}{r_{f2}^2}+k_r\frac{\sin^2\beta}{r_{r2}^2})\right\rangle & \left\langle 2(-ak_f\frac{\sin^2\alpha}{r_{f2}^2}+bk_r\frac{\sin^2\beta}{r_{r2}^2})\right\rangle & -k_f\frac{\sin^2\alpha}{r_{f1}r_{f2}} & -k_f\frac{\sin^2\alpha}{r_{f1}r_{f2}} & -k_r\frac{\sin^2\beta}{r_{r1}r_{r2}} & -k_r\frac{\sin^2\beta}{r_{r1}r_{r2}} \\ & \left\langle (n^2+m^2)(k_f\frac{\sin^2\alpha}{r_{f2}^2}+k_r\frac{\sin^2\beta}{r_{r2}^2})\right\rangle & \left\langle (n-m)(-ak_f\frac{\sin^2\alpha}{r_{f2}^2}+bk_r\frac{\sin^2\beta}{r_{r2}^2})\right\rangle & -nk_f\frac{\sin^2\alpha}{r_{f1}r_{f2}} & mk_f\frac{\sin^2\alpha}{r_{f1}r_{f2}} & -nk_r\frac{\sin^2\beta}{r_{r1}r_{r2}} & mk_r\frac{\sin^2\beta}{r_{r1}r_{r2}} \\ & & \left\langle 2(a^2k_f\frac{\sin^2\alpha}{r_{f2}^2}+b^2k_r\frac{\sin^2\beta}{r_{r2}^2})\right\rangle & ak_f\frac{\sin^2\alpha}{r_{f1}r_{f2}} & ak_f\frac{\sin^2\alpha}{r_{f1}r_{f2}} & -bk_r\frac{\sin^2\beta}{r_{r1}r_{r2}} & -bk_r\frac{\sin^2\beta}{r_{r1}r_{r2}} \\ & & & k_f\frac{\sin^2\alpha}{r_{f1}^2}+k_{fw} & 0 & 0 & 0 \\ & & sym & & k_f\frac{\sin^2\alpha}{r_{f1}^2}+k_{fw} & 0 & 0 \\ & & & & & k_r\frac{\sin^2\beta}{r_{r1}^2}+k_{rw} & 0 \\ & & & & & & k_r\frac{\sin^2\beta}{r_{r1}^2}+k_{rw} \end{pmatrix}$$

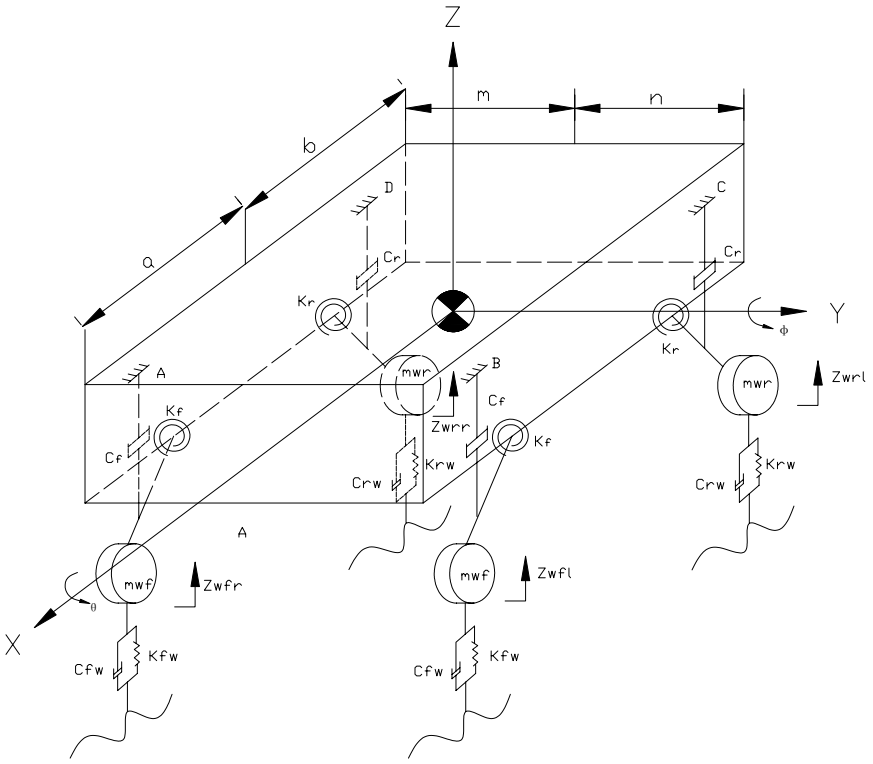


**Fig. 1.** The new 7-DOF spatial vibration model for the planetary wheeled vehicle.

The road excitation vector is $\{F\}=\{F_1\}+\{F_2\}$, where

$$\{F_1\}=[C_W]\{\dot{q}\}=\begin{pmatrix}0&0&0&0\\0&0&0&0\\0&0&0&0\\c_{fw}&0&0&0\\0&c_{fw}&0&0\\0&0&c_{rw}&0\\0&0&0&c_{rw}\end{pmatrix}\begin{pmatrix}\dot{q}_B\\\dot{q}_A\\\dot{q}_C\\\dot{q}_D\end{pmatrix},$$

$$\{F_2\}=[K_W]\{q\}=\begin{pmatrix}0&0&0&0\\0&0&0&0\\0&0&0&0\\k_{fw}&0&0&0\\0&k_{fw}&0&0\\0&0&k_{rw}&0\\0&0&0&k_{rw}\end{pmatrix}\begin{pmatrix}q_B\\q_A\\q_C\\q_D\end{pmatrix}$$

According to literature [2],

$$q_i=\frac{q_{i1}+q_{i2}}{2}\ ,\quad i=B,A,C,D$$

$q_{i1}$ and $q_{i2}$ are the road roughness functions that respectively belong to the front and rear grounded gear of the i[th] planetary wheel, which satisfy the following relationship:

$$q_{i2}(t)=q_{i1}(t-\frac{\sqrt{3}R}{v})$$

The Fourier transform of the above expression is:

$$q_i(f)=\frac{1+e^{-j2\pi f\sqrt{3}R/v}}{2}q_{i1}(f)\ ,\ i=B,A,C,D$$

## 3. The Frequency Characteristics of Vibration System

### 3.1. The Frequency Characteristics of Body Center-of-mass

By the Fourier transform for both sides of the formulation (1), the frequency response function matrix of the system response displacement vector relating to the equivalent road excitation vector is obtained:

$$[H(f)]_{Z\sim q}=\left\{-(2\pi f)^2[M]+j2\pi f[C]+[K]\right\}^{-1}\bullet\left\{[K_W]+j2\pi f[C_W]\right\}\qquad(2)$$

Therefore, the frequency response function matrix of the system response velocity vector relating to the equivalent road excitation vector is obtained:

$$[H(f)]_{\dot{Z}\sim q}=j2\pi f\cdot[H(f)]_{Z\sim q}\qquad(3)$$

The frequency response function matrix of the system response acceleration vector relating to the equivalent road excitation vector is obtained:

$$[H(f)]_{\ddot{Z}\sim q} = (j2\pi f)^2 \cdot [H(f)]_{Z-q} \tag{4}$$

So the frequency response function vector of the displacement of the body center-of-mass relating to the equivalent road excitation vector is the first row of matrix (2). Similarly, the frequency response function vector of the velocity of the body center-of-mass relating to the equivalent road excitation vector is the first row of matrix (3), the frequency response function vector of the acceleration of the body center-of-mass relating to the equivalent road excitation vector is the first row of matrix (4). Since the symmetry of the vehicle structure, the frequency characteristics of the motion of the body center-of-mass relating to the equivalent road excitation are consistent. Without loss of generality, with the frequency characteristics of the motion of the body center-of-mass relating to the road excitation of the equivalent right front wheel in mind, as shown in Fig. 2. When the frequency is 25.42 Hz in the figure of amplitude-frequency characteristics, the system reaches resonance peaks. The steady-state gain of displacement of body center-of-mass relating to road excitation of equivalent wheel is always less than 1, similarly, the steady-state gain of velocity and acceleration of body center-of-mass relating to road excitation of equivalent wheels reach resonance peaks which is the maximum. In the figure of phase-frequency characteristic, the phase values of displacement, velocity and acceleration increase successively by the step of 0.5π, which indicates that phase of acceleration advances 0.5π than phase of velocity, and phase of velocity advances 0.5π than phase of displacement. During (0.001, 90) Hz frequency interval, the phase-frequency curves are across 1.5π, curves turning points are also at the 25.42 Hz. In conclusion of frequency characteristics of the motion of body center-of-mass, vibration parameters of this vehicle avoid the frequency-sensitive interval, which indicates that the parameters are reasonable.

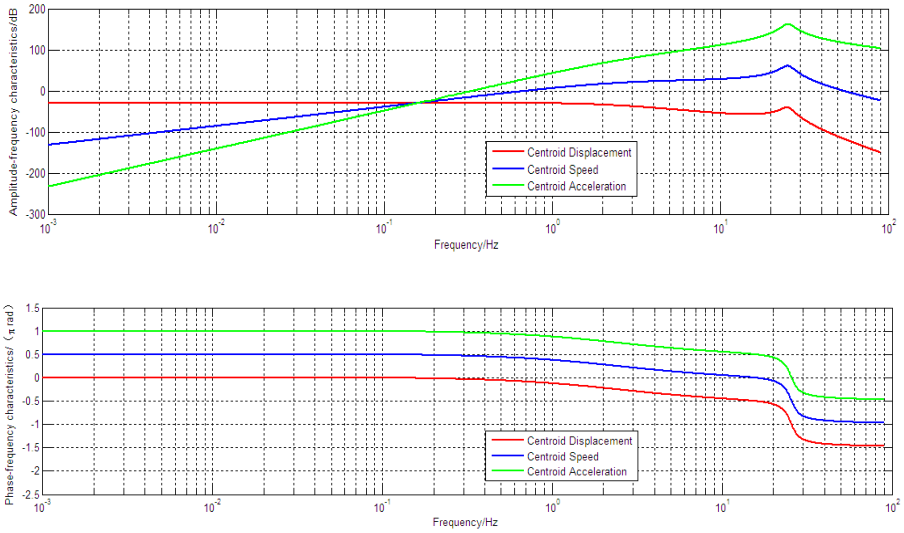


**Fig. 2.** Bode diagram of Body centroid motion for the road surface excitation of the equivalent right front wheel.

## 3.2. Frequency Characteristics of Suspension Dynamic Deflection

Suspension dynamic deflection is expressed as:

$$\begin{cases} f_B = z_B - \dfrac{r_{f2}}{r_{f1}} z_{wfl} = z_M - a\varphi + n\theta - \dfrac{r_{f2}}{r_{f1}} z_{wfl} \\ f_A = z_A - \dfrac{r_{f2}}{r_{f1}} z_{wfr} = z_M - a\varphi - m\theta - \dfrac{r_{f2}}{r_{f1}} z_{wfr} \\ f_C = z_C - \dfrac{r_{r2}}{r_{r1}} z_{wrl} = z_M + b\varphi + n\theta - \dfrac{r_{r2}}{r_{r1}} z_{wrl} \\ f_D = z_D - \dfrac{r_{r2}}{r_{r1}} z_{wrr} = z_M + b\varphi - m\theta - \dfrac{r_{r2}}{r_{r1}} z_{wrr} \end{cases}$$

The Fourier transform of above expression divides by the Fourier transform of the equivalent road excitation to obtain the frequency response function matrix of suspension dynamic deflection relating to equivalent road excitation, as shown as following:

$$[H_{f\sim q}(f)]=[A_f][H(f)]= \begin{pmatrix} 1 & n & -a & -\dfrac{r_{f2}}{r_{f1}} & 0 & 0 & 0 \\ 1 & -m & -a & 0 & -\dfrac{r_{f2}}{r_{f1}} & 0 & 0 \\ 1 & n & b & 0 & 0 & -\dfrac{r_{r2}}{r_{r1}} & 0 \\ 1 & -m & b & 0 & 0 & 0 & -\dfrac{r_{r2}}{r_{r1}} \end{pmatrix} [H(f)] \tag{5}$$

where matrix $[H_{f\sim q}(f)]$ is given in the preceding paragraphs. $[H_{f\sim q}(f)]$ is a 4th-order square matrix. The i[th] row of this matrix is the frequency response function vector of i[th] suspension dynamic deflection relating to the road excitation vector (i = 1,2,3,4 corresponding respectively to the B, A, C, D suspension).

Taking the right front suspension as an example, Bode diagrams of the frequency response functions of these dynamic deflections are shown in Fig. 3. Fig. 3(b) shows the dynamic deflection relating to equivalent road excitation on itself wheel. On the amplitude-frequency curve, the steady-state gain is -30.41 at 0.001 Hz, with frequency increasing successively, the value remains unchanged. There is the peak at 25.17 Hz with the value of 32.94, then, as the frequency increment, it rapidly decays to -51.32 (90 Hz); on the phase-frequency curve, the phase starts with the value of π, finally reduced to 0, while there is the turning point at the same frequency of 25.17Hz. The frequency response curves of this dynamic deflection relating to equivalent road excitation of the other wheels are similar, shown in (a), (c) and (d). With (a) in mind, on the amplitude-frequency curve, the steady-state gain is -30.41 at 0.001 Hz, while at 23.14 Hz, it reaches to -36.97 as a little peak as the body's inertia of being uplifted by the road shock, there is a negative peak that rapidly transits to -93.1 at 25.64 Hz, which is caused by the compressed suspension when the diagonal corner of body is uplifted, and later, it returns to -48.29 at 27.76 Hz, with the frequency increasing, the gain reduces, at 90 Hz, it reaches to -138.2; on the phase-frequency curve, the phase is 0 at 0.001 Hz, and as the same, at 25.64 Hz there is a saltus, which jumps to a higher phase value, then, with frequency increasing, the phase reduces to -1.5π.

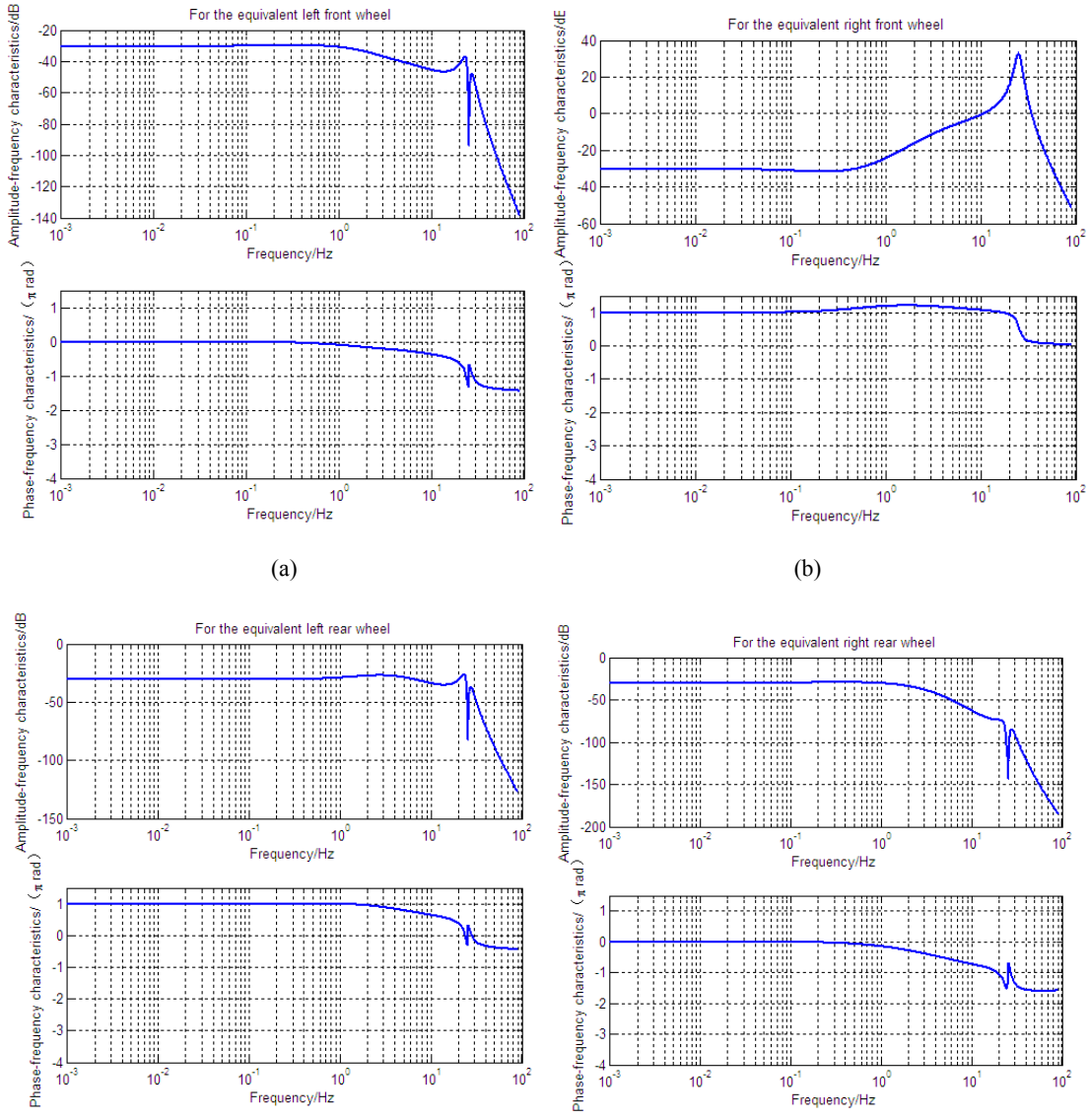


**Fig. 3.** Bode diagram of the right front suspension dynamic deflection for equivalent road excitation vector.

In conclusion of frequency characteristics of the suspensions dynamic deflection, vibration parameters of this vehicle also avoid the frequency-sensitive interval, which indicates that the parameters are reasonable.

### 3.3. Frequency Characteristics of Relative Dynamic Loadings of the Equivalent Wheels

Static loadings of equivalent wheels satisfy the following equilibrium equation:

$$\begin{cases} (G_C^{'} + G_D^{'})(a+b) = Mga \\ (G_C^{'} + G_B^{'})(m+n) = Mgm \\ (G_A^{'} + G_B^{'})(a+b) = Mgb \\ (G_A^{'} + G_D^{'})(m+n) = Mgn \end{cases}$$

Therefore, static loadings of the equivalent wheel are solved:

$$\begin{cases} G_A = m_{wf}g + G_A^{'} = m_{wf}g + Mg\dfrac{b}{a+b}\cdot\dfrac{n}{m+n} \\ G_B = m_{wf}g + G_B^{'} = m_{wf}g + Mg\dfrac{b}{a+b}\cdot\dfrac{m}{m+n} \\ G_C = m_{wr}g + G_C^{'} = m_{wr}g + Mg\dfrac{a}{a+b}\cdot\dfrac{m}{m+n} \\ G_D = m_{wr}g + G_D^{'} = m_{wr}g + Mg\dfrac{a}{a+b}\cdot\dfrac{n}{m+n} \end{cases} \quad (6)$$

The expression of dynamic loadings is described as following:

$$\begin{cases} F_{dA} = m_{wf}\ddot{z}_{wfr} + c_f\dfrac{r_{f2}}{r_{f1}}[\dfrac{r_{f2}}{r_{f1}}\dot{z}_{wfr} - (\dot{z}_M - a\dot{\phi} - m\dot{\theta})] + \\ \quad + k_f\dfrac{sin^2\alpha}{r_{f1}}[\dfrac{z_{wfr}}{r_{f1}} - \dfrac{z_M - a\phi - m\theta}{r_{f2}}] \\ F_{dB} = m_{wf}\ddot{z}_{wfl} + c_f\dfrac{r_{f2}}{r_{f1}}[\dfrac{r_{f2}}{r_{f1}}\dot{z}_{wfl} - (\dot{z}_M - a\dot{\phi} + n\dot{\theta})] + \\ \quad + k_f\dfrac{sin^2\alpha}{r_{f1}}[\dfrac{z_{wfl}}{r_{f1}} - \dfrac{z_M - a\phi + n\theta}{r_{f2}}] \\ F_{dC} = m_{wr}\ddot{z}_{wrl} + c_r\dfrac{r_{r2}}{r_{r1}}[\dfrac{r_{r2}}{r_{r1}}\dot{z}_{wrl} - (\dot{z}_M + b\dot{\phi} + n\dot{\theta})] + \\ \quad + k_r\dfrac{sin^2\beta}{r_{r1}}[\dfrac{z_{wrl}}{r_{r1}} - \dfrac{z_M + b\phi + n\theta}{r_{r2}}] \\ F_{dD} = m_{wr}\ddot{z}_{wrr} + c_r\dfrac{r_{r2}}{r_{r1}}[\dfrac{r_{r2}}{r_{r1}}\dot{z}_{wrr} - (\dot{z}_M + b\dot{\phi} - m\dot{\theta})] + \\ \quad + k_r\dfrac{sin^2\beta}{r_{r1}}[\dfrac{z_{wrr}}{r_{r1}} - \dfrac{z_M + b\phi - m\theta}{r_{r2}}] \end{cases} \quad (7)$$

By the formulation (6), (7), we can obtain the relative dynamic loading $\frac{F_{di}}{G_i}$ of each equivalent wheel, and then obtain the frequency response functions of the relative dynamic loadings of equivalent wheels relating to the road excitations by Fourier transform. Written in matrix form is as following:

$$[H_{\frac{F_{di}}{G_i}\sim q}(f)] = [A_{\frac{F_{di}}{G_i}}(f)][H(f)], \quad (8)$$

where $[H(f)] = [H(f)]_{Z-q}$ the coefficient matrix is recorded as:

$$[A_{\frac{F_{di}}{G_i}}(f)] = \begin{pmatrix} -\Omega_f/G_B & -m\Omega_f/G_B & a\Omega_f/G_B & \Delta_f/G_B & 0 & 0 & 0 \\ -\Omega_f/G_A & m\Omega_f/G_A & a\Omega_f/G_A & 0 & \Delta_f/G_A & 0 & 0 \\ -\Omega_r/G_C & -m\Omega_r/G_C & -b\Omega_r/G_C & 0 & 0 & \Delta_r/G_C & 0 \\ -\Omega_r/G_D & m\Omega_r/G_D & -b\Omega_r/G_D & 0 & 0 & 0 & \Delta_r/G_D \end{pmatrix}$$

Among them,

$$\Delta_f = (i2\pi f)^2 m_{wf} + (i2\pi f)c_f\frac{r_{f2}^2}{r_{f1}^2} + k_f\frac{\sin^2\alpha}{r_{f1}^2}$$

$$\Delta_r = (i2\pi f)^2 m_{wr} + (i2\pi f)c_r\frac{r_{r2}^2}{r_{r1}^2} + k_r\frac{\sin^2\beta}{r_{r1}^2}$$

$$\Omega_f = (i2\pi f)c_f\frac{r_{f2}}{r_{f1}} + k_f\frac{\sin^2\alpha}{r_{f1}r_{f2}}$$

$$\Omega_r = (i2\pi f)c_r\frac{r_{r2}}{r_{r1}} + k_r\frac{\sin^2\beta}{r_{r1}r_{r2}}$$

$[H_{\frac{F_{di}}{G_i}\sim q}(f)]$ is a 4th-order square matrix, The ith row of this matrix is the frequency response function vector of relative dynamic loading of i[th] equivalent wheel relating to the road excitation vector (i = 1, 2, 3, 4 corresponding respectively to the B, A, C, D wheel).

Taking the right rear equivalent wheel as an example, Bode diagrams of the frequency response functions of the relative dynamic loadings of this wheel relating to the four road excitations are shown in Fig. 3. The Fig. 3(d) shows the relative dynamic loading relating to equivalent road excitation on itself wheel. On the amplitude-frequency curve, the stead-state gain is -89.3 at 0.001 Hz, with frequency increasing successively, the value remains unchanged. At 0. 11 Hz, the steady-state gain starts to rise. There is the peak at 25.53 Hz with the value of 114.2, then, as the frequency increment, it rapidly decays to -79.93 (90 Hz); on the phase-frequency curve, the phase starts with the value of 0, and then grows along with the frequency, there is a turning point at 0.11 Hz, later reaches a steady state with the value of 0. 8788π at 12.86 Hz, finally reduced to 0, while there is also a turning point at the same frequency of 25.53 Hz. The frequency response curves of the relative dynamic loadings of this wheel relating to equivalent road excitations of the other wheels are similar, shown in (a), (b) and (c). With (a) in mind, on the amplitude-frequency curve, the steady-state gain is -89.3 at 0.001 Hz, with frequency

increasing successively, the value remains unchanged. while at 0.11 Hz, it starts to rise, there is the first turning point at 0.45 Hz in the rising process, there is the second turning point at 4.62 Hz where the gain reaches a steady state, then it rapidly rises to 62.64 as a peak at 25.53 Hz, later it rapidly reduces to -105.8 (90 Hz); on the phase-frequency curve, the phase is 0 at 0.001 Hz, with frequency increasing successively, the value rises. at 0.11 Hz, there is the first turning point, at 1.13 Hz, it reaches the maximum of 0.4477π, then reduces with the frequency increasing, and as the same, at 25.53 Hz there is a rapid turning point, finally the phase reduces to -2π. In conclusion of frequency characteristics of the relative dynamic loadings, vibration parameters of this vehicle also avoid the frequency-sensitive interval, which indicates that the parameters are reasonable.

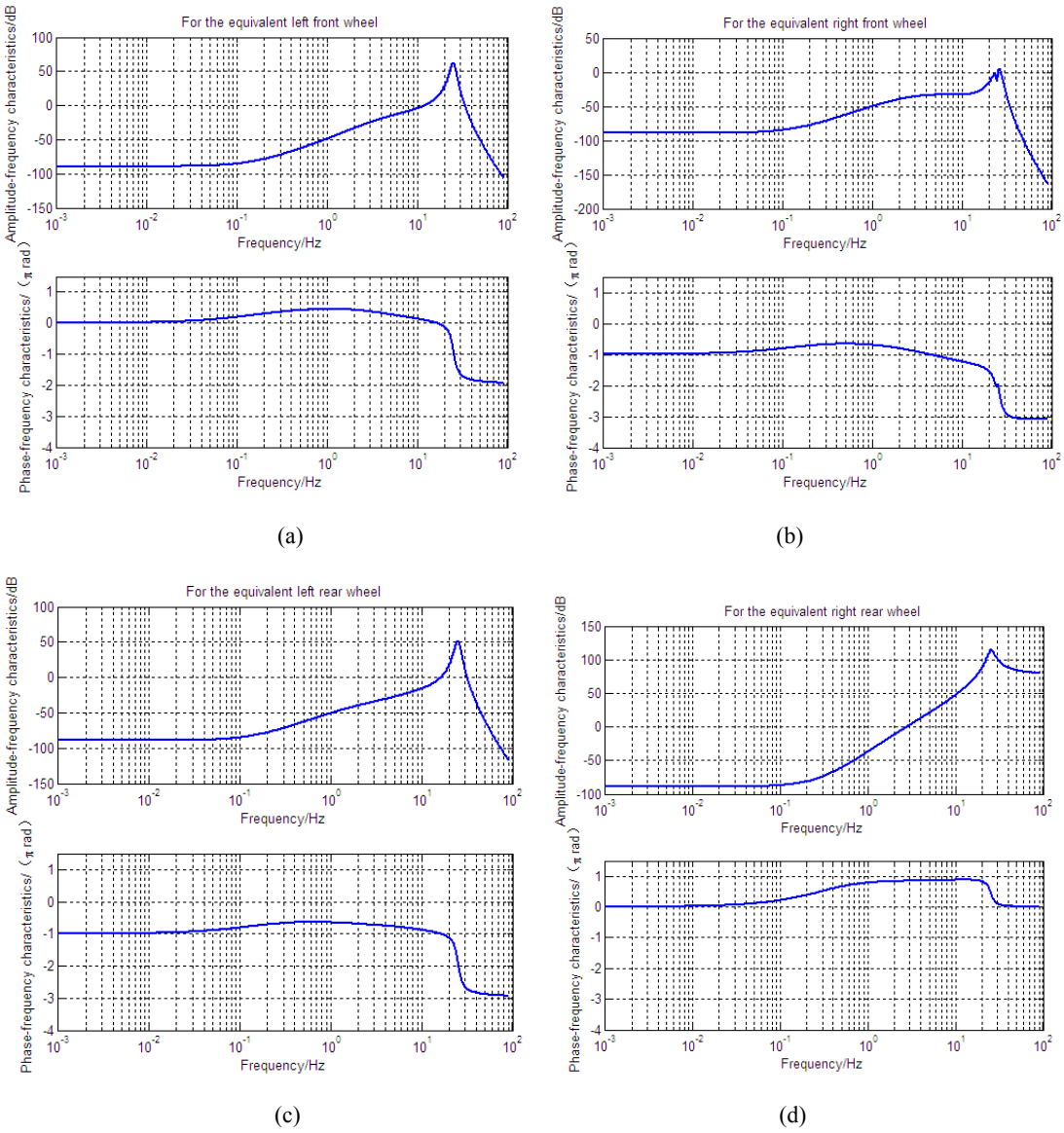


**Fig. 4.** Bode diagram of the right rear equivalent wheel relative dynamic load for equivalent road excitation vector.

## 4. Conclusion

Based on the 7-DOF spatial vibration model of the whole vehicle, differential equations are obtained by Lagrangian equations. Then, the mathematical expressions of the frequency characteristics are derived, the simulation results show that the designed parameters of the vehicle avoid the frequency-sensitive interval, which indicates that the parameters are reasonable, in conclusion of frequency characteristics of the motion of body center-of-mass and the suspensions dynamic deflection and the relative dynamic loadings of the equivalent wheels.

## References

[1]. Weisbin C. R., Rodriguez G., Autonomous rover technology for mars sample return, *in Proceedings of the 5th International Symposium on Artificial*

*Intelligence, Robotics and Automation in Space,* 1999, pp. 1-9.
[2]. Gao Hai-Bo, Deng Zong-Quan, Wang Shao-Chun. Dynamics analysis of the lunar rover with planetary wheel, *Harbin Institute of Technology University,* 37, 1, 2005, pp. 32-35.
[3]. Yu Zhisheng, Vehicle Theory, 4th edition, *Mechanical Industry Press*, Beijing, 2000.
[4]. Li Jie, Qin Yuying, Zhao Qi, The Application of Multi-point Pseudo Excitation Method to Vehicle Random Vibration Analysis, *Automotive Engineering,* 32, 3, 2010, pp. 254-257.